Functional and genomic insights into landfill-isolated *Brucella intermedia* strains capable of degrading Linear Low-Density Polyethylene (LLDPE)

Ifthikhar Zaman[1], Mahdi Muhammad Moosa[1,] *, M. Mahboob Hossain*

Department of Mathematics & Natural Sciences, BRAC University, Dhaka 1212, Bangladesh

[1] *These authors contributed equally to this work*

[1] ifthikhar.zaman@bracu.ac.bd

[1] mahdi.moosa@bracu.ac.bd

[*] *Corresponding Authors*

E-mail: mahdi.moosa@bracu.ac.bd (MMM), mmhossain@bracu.ac.bd (MMH)

Abstract

The global accumulation of linear low-density polyethylene (LLDPE) waste has created an urgent need for sustainable biodegradation strategies. Here, we report the identification and characterization of two *Brucella intermedia* isolates that can degrade LLDPE. Soil samples were collected from the Matuail landfill in Dhaka, Bangladesh, and screened on minimal salt medium supplemented with LLDPE. Both isolates demonstrated growth capacity under carbon-limited conditions, with LLPDE polymer being the sole carbon source. LLDPE polymer samples recovered from bacterial cultures showed extensive chemical and physical alterations as evidenced by Fourier-transform infrared (FTIR) spectroscopy and scanning electron microscopy (SEM), respectively. FTIR spectroscopy analysis of bacteria-incubated plastic sheets showed the formation of new carbonyl, hydroxyl, and ester functional groups consistent with oxidative degradation of plastics. SEM confirmed surface erosion and cracking. Whole-genome sequencing identified both isolates as closely related but distinct strains of *Brucella intermedia* (ANI > 99.5%), enriched in enzymes associated with oxidative activation (copper oxidase), depolymerization (polyesterase, PLA depolymerase, polyamidase), and assimilation-mineralization (3-hydroxyvalerate dehydrogenase). Comparative resistome profiling revealed a stable, efflux-dominated resistance mechanism with RND-type and SMR transporters. Both landfill isolates lacked homologs to known virulence factors, suggesting minimal pathogenic potential. Both isolates exhibited hydrocarbon-induced biofilm formation, supported by the presence of adhesion and exopolysaccharide biosynthesis genes. Collectively, these findings identify environmental *B. intermedia* strains as low-risk, ecologically adapted bacteria capable of LLDPE degradation. This work expands our understanding of plastic-degrading microbes and reveals genomic insights into *Brucella*-mediated LLDPE degradation, advancing our repertoire in plastic bioremediation.

Key Words: *LLDPE biodegradation; plastic-degrading bacteria; environmental biotechnology, whole-genome sequencing; environmental adaptation*

1. Introduction

The global plastic pollution crisis has driven significant research into microbial systems capable of degrading recalcitrant polymers, especially polyethylene (PE). As non-biodegradable plastics, PE-polymers can persist for centuries and enter food chains through contaminated microplastics (Chamas et al., 2020). Recent studies have confirmed the presence of microplastics in human blood, lungs, and placenta, highlighting potential health risks (Leslie et al., 2022; Ragusa et al., 2021). Among all plastic types, the environmental accumulation of PE waste remains a critical global concern due to its high resistance to degradation and widespread use (Gorish et al., 2024). PE's chemical inertness, attributed to the strong C–C and C–H bonds, renders its natural removal from the environment extremely slow.

A variety of PEs are commercially available, with different physical properties and end utilities, including High-Density Polyethylene (HDPE), Low-Density Polyethylene (LDPE), Linear Low-Density Polyethylene (LLDPE), and Polyethylene Terephthalate (PET). Among these, LLDPE is extensively used in food packaging, agricultural films, and household items (Gorish et al., 2024) and therefore, is extensively accumulated. In this study, we focused on LLDPE, one of the most widely utilized PE types globally (Peacock, 2000; Rahimi and García, 2017). LLDPE (Linear Low-Density Polyethylene) is a copolymer primarily composed of ethylene as the main monomer, with small amounts of α-olefins (such as 1-butene, 1-hexene, or 1-octene) as comonomers. These comonomers introduce short-chain branching along the polyethylene backbone, providing distinct properties compared to HDPE. Structurally, LLDPE consists mainly of saturated hydrocarbon chains ($–CH_2–CH_2–$ units), but due to comonomer incorporation, it is not a simple linear alkene. The introduction of short branches decreases crystallinity and increases amorphous regions, thereby enhancing flexibility, tensile strength, and puncture resistance. These characteristics contribute to the wide application of LLDPE in films, stretch wraps, and pouches (Peacock, 2000).

Plastic pollution has emerged as a worldwide environmental issue due to its insufficient recycling and extensive day-to-day usage. Presently, both chemical treatments and bioremediation are employed to address plastic contamination (Omokhagbor Adams et al., 2020). However, chemical approaches often pose environmental risks. As a result, advances in microbial biotechnology have prompted research into isolating microorganisms that degrade plastics from polluted environments such as landfills and waste disposal sites. Bioremediation offers an environmentally friendly solution. by utilizing organisms such as bacteria, fungi, algae, or insects (Thirumalaivasan et al., 2024; Zaman et al., 2024). These bioremediation agents are used to break down, eliminate, transform, stabilize, or neutralize plastic pollutants in the environment (Omokhagbor Adams et al., 2020). Recent studies have focused on isolating bacteria capable of metabolizing polyethylene when provided as the sole carbon source (Alamer et al., 2023). Plastic-degrading bacteria constitute a taxonomically diverse group capable of converting synthetic polymers into less harmful compounds through enzymatic reactions. They secrete extracellular and intracellular enzymes such as depolymerases, hydrolases, oxidoreductases, cutinases, amidases, and esterases, which catalyze the hydrolysis or oxidation of chemical bonds within polymer chains (Atanasova et al., 2021; Bahl et al., 2021).

The biodegradation process typically follows several distinct stages. Three major sequential steps can be easily identified in plastic degradation: oxidation, depolymerization, and assimilation/mineralization. Initially, biodeterioration occurs as microbes and abiotic factors modify the plastic's surface, often facilitated by biofilm formation. Oxidation (initiated by abiotic factors such as UV, heat, or mechanical stress as well as catalyzed by microbial enzymes) introduces oxygen-containing functional groups (*e.g.*, carbonyls, hydroxyls) into the polymer backbone, increasing hydrophilicity and creating cleavage sites for enzymes (Bahl et al., 2021). At this stage, formation of biofilms likely enhances microbial adhesion to surfaces, thereby increasing the efficiency of enzymatic attack on the polymer. Following oxidation, depolymerization occurs when extracellular enzymes (depolymerases, hydrolases, oxidoreductases) cleave the oxidized polymer into oligomers and monomers that are small enough for transport across the cell envelope. After that, assimilation allows these molecules to traverse the microbial membrane, where they are metabolized into energy and biomass. Finally, mineralization converts assimilated compounds into inorganic end products such as CO_2 and H_2O (or CH_4 under anaerobic conditions), completing the degradation process (Bahl et al., 2021; Cai et al., 2023).

Plastic-degrading bacteria identified to date differ in their capabilities, with different species and strains exhibiting varying efficiencies in degrading specific polymers. For example, previous studies report that *Bacillus* species such as *B. amylolyticus* and *B. subtilis* reduce the weight of PE samples significantly (Galgali et al., 2002; Nowak et al., 2011). Likewise, *Pseudomonas putida* demonstrated a high PE degradation rate, reducing plastic mass within short incubation periods (Rajandas et al., 2012). A major advancement was the discovery of an *Ideonella sakaiensis* isolate, which produces PETase and MHETase enzymes capable of breaking down PET into assimilable monomers (Yoshida et al., 2016a). Other genera, such as *Rhodococcus*, *Klebsiella*, and *Acinetobacter,* have also been implicated in polyethylene degradation, though often with lower efficiency than *Pseudomona*s and *Bacillus* species (Ghatge et al., 2020; Skariyachan et al., 2016). Even gut bacteria within an insect species (*Zophobas atratus*) that are fed plastics can use these plastics (LDPE, LLDPE, EPS) as their carbon source (Zaman et al., 2024).

While many studies have reported diverse bacterial species in plastic degradation, this study is the first to provide a whole-genome analysis of *Brucella intermedia* strains exhibiting LLDPE-degrading capacity. Unlike commonly reported plastic degraders such as *Pseudomonas* or *Bacillus*, *Brucella* is traditionally recognized as a pathogenic genus (Qureshi et al., 2023). Our findings, therefore, highlight an unexpected ecological role of *B. intermedia*, suggesting that its metabolic repertoire may extend beyond host interactions to include polymer degradation. This not only expands the known diversity of plastic-degrading bacteria but also opens new avenues for exploring unconventional microbial candidates in biotechnological applications.

2. Materials and methods

2.1 Soil bacteria isolation

Soil samples were collected from the Matuail Sanitary landfill site (latitude 23º43.35' and 23º42.97' N and longitude 90º26.83' and 90º27.2' E) in Dhaka, Bangladesh, to isolate potential LLDPE-degrading bacterial strains ***(SI Figure 1)***. Each sample (1 g) was suspended in 10 mL of sterile 0.9% NaCl solution and subjected to serial dilution. From each dilution, 100 µL was plated onto Minimal Salt Agar (MSA), which is a selective medium. The composition of MSA was as follows: KH_2PO_4 (3 g/L), K_2HPO_4 (0.1 g/L), NaCl (5 g/L), NH_4Cl (2 g/L), $MgSO_4 \cdot 7H_2O$ (0.16 g/L), $CaCl_2 \cdot 2H_2O$ (0.1 g/L), and Agar (2%) with the pH adjusted to 6.5. The medium was sterilized by autoclaving at 121°C for 15 minutes under 15 psi pressure. This medium lacked any organic carbon source. To enable the selection of LLDPE-degrading bacteria, sterilized LLDPE strips were placed on the agar surface after cooling. To sterilize the plastic strips, manufacturer-labeled LLDPE films were washed, cut into uniform strips, and sterilized by soaking in 70% ethanol, as per previous studies (Gupta and Devi, 2020). Controls included: (i) MSA with LLDPE but no bacterial inoculum, and (ii) MSA with inoculum but no LLDPE. Plates were incubated at 37°C for 7 days.

Colonies that emerged at or near the LLDPE film edges were presumed candidates for LLDPE degradation. These isolates were individually streaked onto Nutrient Agar (NA) for purification and further cultured in Minimal Salt Broth (MSB), where LLDPE served as the sole carbon source. In each 250 mL Erlenmeyer flask, sterile LLDPE strips were introduced along with 100 mL of MSB and a single bacterial isolate. Controls included MSB with LLDPE only (no inoculum) and MSB with the isolate only (no LLDPE). All systems were incubated at 37°C and 180 RPM for 60 days.

Throughout the incubation, Colony Forming Unit (CFU) estimation was monitored at 7-day intervals using OD_{600} readings (data not shown). At the end of the 60-day incubation, these cultures were sub-cultured on NA, and LLDPE films were recovered for Fourier Transform Infrared Spectroscopy (FTIR) and Scanning Electron Microscopy (SEM) to evaluate structural degradation. Isolates that showed growth on LLDPE were selected for further biofilm assays, 16S rRNA gene sequencing, and whole genome sequencing (WGS).

2.2 Fourier Transform Infrared Spectroscopy (FTIR)

FTIR (IRPrestige-21, SHIMADZU, Japan) was used to prove biodegradation by analyzing the new functional group formed in the LLDPE. 60 days incubated LLDPE with the isolates was used as a sample, where a fresh LLDPE acted as a control. FTIR was done as previously described (Singh et al., 2012).

2.3 Scanning Electron Microscopy (SEM)

SEM was performed on the treated LLDPE with both isolates. SEM was performed using an ultra-high-resolution Schottky Field Emission Scanning Electron Microscope (JSM-7610F, JEOL, Japan). Images were taken after LLDPE samples were incubated in MS broth with isolated bacteria for two months. Untreated LLDPE was used as a control. After incubation, samples were prepared as previously described (Taghavi et al., 2021). Images were captured at 1µm length with 3000x magnification.

2.4 Biofilm analysis

To assess the biofilm-forming potential of the isolates under both nutrient-rich and hydrocarbon-substituted conditions, two types of qualitative biofilm assays were performed using the Congo Red Agar (CRA) method, following the protocol with modifications (Freeman et al., 1989).

In the first condition (standard CRA), the medium consisted of Brain Heart Infusion (BHI) broth (37 g/L), sucrose (50 g/L), agar (15 g/L), and Congo red dye (0.8 g/L). For the second condition (modified CRA), the BHI broth was replaced with hexadecane (100 µL/100 mL), while keeping the concentrations of sucrose, agar, and Congo red dye constant. Both solid and liquid forms of these media were prepared to observe biofilm formation in agar plates and broth conditions, respectively. Notably, the broth system contained a higher effective concentration of hexadecane due to increased availability in the liquid phase.

All assays were conducted with appropriate positive and negative controls. For the modified CRA, media with and without hexadecane were incubated for 24 and 48 hours to assess time-dependent biofilm formation. The interpretation criteria were as follows: colonies exhibiting black coloration or black precipitation on CRA plates or in broth were considered positive for strong biofilm formation, whereas colonies remaining red or pink without black precipitation were classified as non-biofilm producers.

2.5 Whole genome sequencing and assembly

Raw Oxford Nanopore Technologies (ONT) reads were processed using a custom Snakemake workflow. Initial taxonomic classification was performed using Kraken2 (v2.0.8-beta), and reads assigned to predefined contaminant taxa were removed using seqkit grep (SeqKit, v2.10.0) (Shen et al., 2024; Wood et al., 2019). Read quality was evaluated using NanoPlot (v1.44.1), and filtering was conducted with NanoFilt (v2.8.0), retaining reads with minimum length of 1000 bp and average quality ≥10 (De Coster et al., 2018). Filtered reads were assembled de novo using Flye (v2.9.5) with an estimated genome size of 5 Mb (Kolmogorov et al., 2019). Genome/chromosome circularity status was inferred from Flye output. Assembly polishing was performed in two stages: three iterative rounds of Racon (v1.5.0), followed by consensus refinement with Medaka using the model r1041_e82_260bps_hac_v4.1.0. Assembly completeness was evaluated with BUSCO (v5.8.3) 5 using the bacteria_odb12 dataset (Manni et al., 2021). Assembly quality and structural metrics were further assessed using QUAST (v5.0.2). Sequencing depth was estimated by aligning filtered reads to the polished assembly using Minimap2 (v2.26), followed by sorting, indexing, and coverage computation with SAMtools (v1.21) using samtools coverage.

2.6 Taxonomic Assignment and Reference Genome Retrieval

Whole-genome assemblies of the two bacterial isolates, designated X and Y, were initially taxonomically classified using Kraken2 v2.0.8-beta with the pluspf16 Kraken2 database. Both genomes were confidently assigned to the genus *Brucella*. Independently, 16S RNA sequences of both bacterial isolates also indicated that both isolates belonged to the *Brucella* genus. To identify appropriate reference genomes for comparative analysis, all complete genome assemblies of the genus *Brucella* were retrieved from the NCBI RefSeq database (date: May 14, 2025). Only assemblies at the "Complete Genome" level were included to ensure consistency and high sequence quality (n = 231).

2.7 Average Nucleotide Identity (ANI) Screening & Isolate Difference Assessment

Species-level classification was refined using FastANI v1.1, which calculates pairwise Average Nucleotide Identity (ANI) between query and reference genomes (Jain et al., 2018). Genomes of isolates X and Y were also compared with each other using reciprocal Minimap2–Medaka (v2.0.1, model: r1041_e82_260bps_hac_variant_v4.1.0_model_pt.tar.gz) variant calling and whole-genome alignment with MUMmer v3.23 (dnadiff/nucmer).

2.8 Whole genome comparison

Whole-genome relationships among representative *Brucella* isolates were assessed using Mashtree (v1.4.6) (Katz et al., 2019). Complete and representative *Brucella* genomes from NCBI, spanning both pathogenic and environmental lineages, were analyzed alongside the study isolates X and Y *(SI Table 1)*. The resulting distance matrix was converted to a neighbor-joining tree, midpoint-rooted, and visualized in ETE3 (v3.1.3) (Huerta-Cepas et al., 2016), with branch-lengths square-root–scaled and species names mapped from NCBI metadata.

For focused genome comparison, each landfill isolate (X and Y) was mapped to the closest high-quality *B. intermedia* reference genome (GCF_048398275.1; hospital-wastewater origin). For every annotated CDS in the reference, their presence-absence in the landfill isolates and relocation status were checked. A CDS was called absent if <80% of its length was covered at the native locus and no relocated match was detected in the isolate assembly (≥80% query coverage, ≥90% amino acid identity). Consecutive absent CDS located <5 kb apart on the same reference contig were merged into genomic "accessory islands." Genomic span, GC content, number of CDS, and representative annotations were checked for each of the islands. These islands were visualized as depth dropouts in a circular genome plot, rendered from whole-genome alignments and coverage tracks using minimap2, samtools, and pyCirclize. Complete calling criteria, coordinates, and functional summaries are provided in *SI Note 1* and *SI Table 2*.

2.9 Pairwise variant identification and visualization

Single nucleotide polymorphisms (SNPs) and small insertions/deletions (indels) between the landfill isolates (X and Y) were identified using Snippy v4.6.0 (Seemann, 2025a), with the Y isolate assembly as the primary reference. Variants were parsed from the resulting VCF file, classified as SNP or indel, binned by a 100 bp genomic coordinate, and plotted as a stacked lollipop plot using Matplotlib v3.9 using a custom *in-house* Python script. In the stacked lollipop plot, each stick represents local variant pile-up along the two chromosomes of the reference genome(s) (GCF_043898275.1 for *Figure 3C* and the Y isolate genome for *SI Figure 2*). SNPs and indels were visualized together as stacked lollipop plots to illustrate overall genome-wide variation. In SI Figure 2, these were shown separately to distinguish variant types across the two chromosomes. The region absent in X (2.255–2.275 Mb) was further examined using the corresponding locus from the closest published *B. intermedia* reference genome (GCF_043898275.1; *SI Figure 2C*); gene models were extracted directly from its NCBI GFF annotation file to indicate gene content and putative functions

2.10 Identification of plastic-degrading genes

Genome assemblies (FASTA format) were screened with an in-house workflow. Protein-coding genes were predicted using Prokka v1.14.6 (default settings). The resulting proteins were queried against PlasticDB (May 18, 2025 release) with BLASTP v2.16.0 (E-value $\leq 1 \times 10^{-5}$) (Gambarini et al., 2022). A match was accepted when (i) amino-acid identity ≥ 30 %, (ii) query coverage ≥ 60 %, and (iii) subject coverage ≥ 60 %. BLAST hits were parsed to extract enzyme annotations from the target sequence identifiers, which encoded enzyme names in a delimiter-separated format. Enzyme counts were summarized per genome, and individual summaries were aggregated into a master count matrix for comparative analysis.

2.11 Resistome and virulence factor prediction

Antimicrobial resistance and virulence-associated genes were identified using ABRicate on the Galaxy (U.S.) server (Afgan et al., 2018; Seemann, 2025b) with the ResFinder (Zankari et al., 2012) and VFDB databases (≥70% identity, ≥80% coverage) (Chen et al., 2016). Additional resistance analysis was performed using the Comprehensive Antibiotic Resistance Database (CARD) via the Resistance Gene Identifier (RGI) web interface (Alcock et al., 2023).

2.12 Biofilm-forming gene prediction

A curated dataset of 63 biofilm-associated proteins was compiled from experimentally validated systems across diverse microorganisms, including *Staphylococcus aureus*, *Pseudomonas aeruginosa*, *Escherichia coli*, *Vibrio cholerae*, *Bacillus subtilis*, *Enterococcus faecalis*, and *Candida albicans* through conducting a literature survey **(***SI Table 3***)**. These reference proteins represent core components of adhesion, matrix biosynthesis, quorum-sensing, and regulatory networks involved in biofilm formation. Protein sequences were obtained from UniProt and used as a BLASTp query set against the predicted proteomes of *Brucella* landfill isolates X and Y.

3. Results and discussion

3.1 Landfill microbiota harbor LLDPE-degrading bacterial isolates

Following a 7-day incubation on MSA plates containing LLDPE, 4-5 distinct colony morphotypes were observed growing adjacent to the LLDPE film margins. In contrast, the negative control plate containing LLDPE without soil inoculum exhibited no visible growth, confirming the sterility of the LLDPE and the selectivity of the medium. Plates containing only the soil sample (without LLDPE) did show multiple colonies, as expected due to the presence of native soil microbes. To further validate potential LLDPE degraders, all colonies from MSA plates with both LLDPE and inoculum were individually purified on Nutrient Agar and subsequently inoculated into Minimal Salt Broth (MSB) with LLDPE as the sole carbon source. CFU counts were tracked every 7 days using OD_{600} measurements (data not shown). After 60 days, only two isolates showed significant CFU increases compared to their initial counts, suggesting active proliferation using LLDPE.

To reduce false positives and assess long-term viability, all systems were sub-cultured in NA after day 60. In systems containing only the isolates (no LLDPE), no growth was observed beyond day 7, indicating that the bacteria could not survive in the absence of an external carbon source. Similarly, the uninoculated LLDPE control flasks remained sterile throughout the 60-day period. These results confirm that only two isolates demonstrated the ability to utilize LLDPE as the sole

carbon source under the given conditions. As a result, the initial growth observed during the first incubation may have been the result of residual organic matter in the soil or media (or dead bacteria), potentially leading to initial false positives. However, the extended incubation in MSB, a strictly inorganic medium, and subsequent lack of growth in control systems confirmed the validity of the two true LLDPE-degrading strains, designated isolates "X" and "Y". The recovered LLDPE films from these two systems were subjected to FTIR and SEM analyses to assess chemical and surface-level degradation.

The selective isolation of only two degraders from numerous initial colonies highlights the rarity of microbes with authentic LLDPE-degrading capacity. This is consistent with previous reports, where only a small fraction of soil or landfill microbiota demonstrated the ability to utilize polyethylene as the sole carbon source. Moreover, extended incubation in MSB medium is particularly important, as it reduces the risk of false positives that may arise from residual organic matter, and it ensures that only strains with genuine metabolic potential for plastic degradation are identified. Furthermore, the growth and degradation of LLDPE indicate specialized metabolic adaptations. Similar findings have been reported in other species, where oxidative enzymes and biofilm-associated proteins enabled survival under carbon-limited, polymer-dependent conditions (Skariyachan et al., 2016). This suggests that isolates X and Y may employ comparable oxidative and/or hydrophobic interaction strategies. Ecologically, as plastic pollution accumulates in the environment, plastic-degrading bacteria may gain increased access to substrates, enabling greater energy acquisition, growth, and persistence. Landfill environments, rich in hydrocarbons and recalcitrant polymers, can act as hotspots for the emergence of microbial populations with specialized plastic-degrading capabilities.

3.2 Activities of plastic-degrading bacterial isolates induce chemical changes in LLDPE

It was previously reported that microbial degradation of plastics results in chemical alterations (Gautam et al., 2007). To check whether our landfill bacterial isolates induce chemical changes upon incubation, we performed FTIR analysis of LLDPE samples after bacterial incubation. Our FTIR data demonstrates that distinct functional groups were formed in the bacteria-treated LLDPEs (*Figure 1*) that were absent in the control. The control LLDPE exhibited only the characteristic C–H stretching and a weak band at ~1020 cm^{-1} (C–N stretch), which likely originated from polymer additives or processing residues. In contrast, several new functional groups, for example, 1550-1720 cm^{-1} (C=O stretch), 1250–1300 cm^{-1} (C─O stretch) wavenumbers, were formed by both X and Y isolates in addition to the persistent C–N band. Lastly, a 3000-3670 cm^{-1} (O─H stretch) wavenumber was also found in the treated plastics, but not in the control, consistent with oxidative modification of the polymer backbone. These observations strongly suggest that microbial activity facilitated oxidative changes of the LLDPE surface. The selective emergence of these groups under carbon-limited conditions (MSB medium with LLDPE as the sole carbon source) provides strong evidence for biodegradation activity by both isolates.

The characteristic wavenumbers of the chemical bonds were referenced from previous studies (Socrates, 2004). The broad O–H stretching band observed in the treated samples suggests the formation of alcohol or hydroxylated intermediates, while the carbonyl signal at ~1700 cm^{-1} likely represents ketones, aldehydes, or carboxylic acids formed during polymer oxidation. The presence

of C–O stretching further supports the possibility of ester or ether linkages as oxidative intermediates. Importantly, these groups were completely absent in the untreated control, ruling out abiotic or additive-derived oxidation as the source. Although both isolates exhibited similar patterns of oxygenated functional group formation, subtle differences in peak intensity may reflect variation in their degradation efficiency. These observations align with earlier reports where the appearance of carbonyl (C=O), hydroxyl (O–H), and ester/ether (C–O) peaks was considered a hallmark of microbial polyethylene degradation (Khumthong et al., 2025). Oxidation introduces polar functional groups into the inert polyethylene backbone, thereby increasing hydrophilicity, reducing crystallinity, and making the polymer more accessible to enzymatic depolymerization.

The emergence of O–H and C=O bands in Figures 1B and 1C indicates that the initial step of oxidative biodegradation is underway, which corresponds well with the "oxidation-depolymerization-assimilation" model of plastic degradation. Once oxidative groups are incorporated, extracellular enzymes such as oxidases, peroxidases, and hydrolases can cleave the modified polymer into oligomers or monomers that are then assimilated (Atanasova et al., 2021). This suggests that both isolates X and Y follow a classical oxidative activation mechanism, though the subtle peak intensity differences hint at variable efficiency or enzyme expression between the two strains (*Figure 1*). Interestingly, the persistence of the C–N band across all treatments indicates that certain additive-derived features of commercial plastics may mask or complicate biodegradation signals. This observation reinforces the importance of combining FTIR with complementary analyses, such as weight loss, surface morphology (SEM/AFM), or thermal property changes (TGA/DSC), to build a more comprehensive picture of microbial plastic degradation. In summary, according to the FTIR analysis, both isolate X and Y actively modify the chemical structure of LLDPE through oxidative processes, a crucial prerequisite for polymer fragmentation and subsequent microbial assimilation.

3.3 Activities of plastic-degrading bacterial isolates alter LLDPE surface morphology

Chemical changes happen at the molecular scale. To check whether bacterial isolate-mediated chemical alterations of the LLPDE sample are coupled to physical changes of the LLDPE surface, we directly visualized bacteria-treated-plastic surface using SEM experiments. Our scanning micrograph revealed clear differences in the surface morphology of LLDPE films incubated with isolates X and Y compared to the untreated control (*Figure 2A vs. 2B, 2C*). After 60 days of incubation, the control film maintained smooth and intact surfaces, whereas the treated samples displayed clear degradation signatures, including roughened textures, fissures, and surface fragmentation. Such morphological alterations are consistent with previous observations on microbial plastic degradation, where bacterial colonization and enzymatic action gradually erode the polymer surface (Kyaw et al., 2012; Shah et al., 2008). The roughness and cracking observed on the LLDPE surfaces likely result from extensive oxidative modification of the polymer backbone, as supported by our FTIR findings (*Figure 1*). These surface defects enhance microbial adhesion by increasing surface area, further exposing oxidized functional groups, and thereby facilitating enzymatic depolymerization. Similar SEM-based observations have been reported in other bacterial strains grown on polyethylene films, where extensive pitting, grooves, and cavities indicated microbial attack (Skariyachan et al., 2016).

3.4 Whole genome analysis of plastic-degrading isolates

For species-level identification and a clear understanding of the genetic basis of LLPDE-degrading capacities, we performed whole-genome shotgun sequencing of the two landfill isolates. DNA samples from individual bacterial isolate pure colonies were sequenced, read assembled, and annotated for detailed genomic characterization. Taxonomic classification using Kraken2 indicated that both bacterial isolates belong to the *Brucella* genus. For species identification, we compared assembled X and Y isolate genomes against all available high-quality *Brucella* reference genomes. Both X and Y isolates showed high average nucleotide identity (ANI) scores against previously reported *B. intermedia* genomes (*SI Table 6*). To further delineate isolate taxonomic identities, we performed whole-genome phylogenetic analysis with representative *Brucella* genomes. Results of the phylogenetic analysis showed that both X and Y isolate genomes cluster with other previously sequenced *B. intermedia* isolates (*Figure 3A*). Quite interestingly, we observe that all environmental isolates cluster together (*Figure 3A; SI Table 6*), confirming their close genomic affinity and environmental origin. The whole-genome phylogenetic analysis reveals a clear separation between classical pathogenic and environmental clades, reflecting the evolutionary divergence between host-adapted and free-living *Brucella* lineages (*Figure 3A*).

The whole genome phylogenetic tree showed that both X and Y isolates are close to an environmental *B. intermedia* isolate (GCF_048398275.1; a hospital wastewater isolate from Ghana), with ANI scores of 99.56 and 99.59, respectively (*SI Table 6*). Such a high ANI is typically observed among isolates of the same species or very closely related strains. To directly visualize similarities/differences between the GCF_048398275.1 isolate and X-Y isolates, we compared identities of the landfill isolates *vs.* the nearest reference genome. Whole genome alignment showed that X and Y isolates are largely syntenic but lack discrete multi-gene cassettes that appear in the reference wastewater isolate (*Figure 3B*). These "accessory islands" include phage/plasmid modules and a high-GC (~0.62–0.63) stress/repair block (~2.16–2.22 Mb in the reference) encoding MarR/LysR-family regulators and MsrB, all absent from both landfill isolates (*SI Note 1*).

To characterize the difference between the two landfill isolates, we checked the ANI scores when X and Y are compared with each other. Our analysis revealed that X and Y share a high degree of similarity with ANI scores >99.98. To check whether X and Y are clonally identical, isolate X was directly aligned with isolate Y (*Figure 3C*). A total of 304 single-nucleotide polymorphisms (SNPs) and 160 indels were identified. These variations are uniformly distributed across the two *B. intermedia* chromosomes, without evidence of localized hypermutation. Notably, we also detect a smaller locus present in Y but missing in X that encodes a predicted two-component histidine kinase/sigma factor pair and envelope glycosylation genes (*Figure 3B, SI Figure 2C, SI Table 2*). Together, these differences confirm that the two landfill isolates are closely related but genomically distinct lineages of *B. intermedia*, consistent with microevolution within a shared environmental niche.

To understand the molecular basis of plastic-degrading capacity, we compared these isolates' annotation-derived proteomes against a manually curated set of plastic-degrading proteins (Gambarini et al., 2022). For both isolates, 42 putative plastic degraders were identified (*SI Table*

4). These enzymes represented all key steps in plastic biodegradation (namely, oxidative activation, depolymerization, and assimilation/mineralization). To check whether these genes are significantly enriched vis-à-vis the *Brucella* reference genome background, we determined baseline counts (mean ± standard deviation) for each of these enzymes within publicly available *Brucella* genomes and compared them with identified plastic-degrading genes from X and Y isolates (*Table 1*). Relative to the reference *Brucella* genomes, isolates X and Y were strongly enriched in oxidative activation capacity, moderately enriched in depolymerization enzymes, and showed a near-baseline assimilation potential. Our observations mirror previous reports on plastic-degrading enzyme category expansions in known plastic degraders [*Rhodococcus* spp. (oxidative activation) and *Ideonella* (depolymerization)] (Santo et al., 2013; Yoshida et al., 2016b; Zampolli et al., 2023).

Genomic profiling of the identified enzymes revealed a distinct enrichment pattern across the three major stages of plastic biodegradation: oxidative activation, depolymerization, and assimilation/mineralization (*Table 1*). Among the oxidative activation genes, copper oxidase was strongly overrepresented in both landfill isolates (Z = 8.7). The overabundance of copper oxidase suggests that *B. intermedia* X and Y rely primarily on copper-dependent oxidation to initiate polymer attack. Copper oxidases are known to catalyze electron transfer reactions that introduce carbonyl and hydroxyl functionalities onto hydrocarbon chains, thereby enhancing hydrophilicity and enabling subsequent enzymatic cleavage (Santo et al., 2013). This abundance of oxidative enzyme gene is consistent with our FTIR observations where prolonged incubation of LLDPE polymers with both landfill isolates result in strong carbonyl and hydroxyl peaks (*Figure 1*) that are hallmarks of oxidative changes. We also observed a moderate enrichment of depolymerization genes (Table 1). Both isolates encoded PLA depolymerase, polyesterase, and polyamidase, each showing counts above or equal to the mean reference values. The presence of multiple ester- and amide-cleaving enzymes indicates the likely capacity of the isolates to fragment oxidized polymers through hydrolytic cleavage. Polyamidase and polyesterase are particularly important for breaking secondary amide and ester bonds, while PLA depolymerase suggests broader substrate tolerance extending to aliphatic polyester structures (Shalem et al., 2024). The absence of PHA, PU, and other hydrolases may reflect substrate specialization rather than general loss of function. Together, these genes support efficient depolymerization following an initial oxidation step. Lastly, the assimilation/mineralization stage showed near-baseline or slightly elevated enzyme representation relative to the Brucella reference genomes. Previous studies have reported plastic-degrading capacities of multiple *Brucella* spp, including *B. intermedia* (Alamer et al., 2023; Srivastava et al., 2025), which aligns with the genomic evidence presented here and suggests that these strains have adapted to environmental niches rich in hydrocarbon or polymer substrates. Building on this, we next analyzed their resistance and virulence profiles to evaluate ecological fitness and biosafety.

Combined resistome profiling using the Comprehensive Antibiotic Resistance Database (CARD; RGI; Alcock et al., 2023) and ResFinder (ABRicate; Seemann, 2020) revealed that both X and Y genomes possess an almost identical antimicrobial resistance repertoire. Each genome encodes three RND-type efflux pumps (adeF-like), a small multidrug resistance (SMR) efflux transporter (qacG-like, with a secondary match to qacJ), and an aminoglycoside adenylyltransferase [ANT(9)-Ic] (*SI Table 5*). Screening with ResFinder further identified a class C (AmpC) β-lactamase,

blaOCH-2–like, in both genomes (≈99.5% coverage, ≈83% identity). The high concordance between CARD and ResFinder results indicates a stable, efflux-dominated resistome complemented by enzymatic inactivation mechanisms against aminoglycosides and β-lactams. On the other hand, virulence factor screening using ABRicate (VFDB) detected only loci related to lipopolysaccharide (LPS) and cyclic β-1,2-glucan biosynthesis (kdsA/B, pgm, cgs, acpXL, manCoAg, manAoAg, wbpZ, htrB, fabZ) and the intracellular survival factor ricA. These are conserved structural or stress-response genes found across non-pathogenic *Brucella* /*Ochrobactrum* lineages and are not indicative of pathogenic potential. No homologs of classical virulence determinants (toxins, adhesins, or secretion systems) were detected, supporting the classification of both isolates as low-pathogenic environmental variants.

The observed resistance gene profile indicates that both *B. intermedia* isolates are environmentally resilient and well-adapted to the stress conditions commonly found in soil and landfill ecosystems. Dominant RND and SMR pumps indicate efflux-mediated detoxification that may extend beyond antibiotics to organic solvents and certain aromatic hydrocarbons that maybe generated during plastic biodegradation. Before the widespread use of antibiotics, RND efflux pumps likely evolved to help bacteria detoxify naturally occurring compounds in their environment. The ability to pump out antibiotics is considered an evolutionary novelty that stems from their original function (Alvarez-Ortega et al., 2013). The presence of a chromosomal class C β-lactamase (blaOCH-2–like) is consistent with intrinsic β-lactam resistance typical of environmental *Brucella/Ochrobactrum* lineages (Li et al., 2021; Nadjar et al., 2001), suggesting a baseline tolerance to many penicillins and cephalosporins. This pattern likely reflects environmental adaptation rather than recent clinical antibiotic exposure. This is further supported by the virulence factor profiles of the two landfill isolates, as only conserved structural and stress-responsive virulence genes were detected. Loci involved in LPS and cyclic β-1,2-glucan biosynthesis and the intracellular survival factor ricA play roles in cell envelope integrity and osmotic stress tolerance rather than host infection (Byndloss and Tsolis, 2016). In addition, the complete absence of virulence-associated secretion systems, adhesins, or exotoxins clearly distinguishes these isolates from pathogenic *Brucella* strains (Byndloss and Tsolis, 2016). Together, the resistome and virulome data suggest that isolates X and Y possess a stable, efflux-dominated abiotic resistance mechanism coupled with minimal pathogenic potential. This combination supports potential safe use of these landfill isolates as biodegraders capable of withstanding the physicochemical challenges of plastic-rich habitats without posing health risks.

3.4 LLDPE-degrading Brucella isolates form biofilms on plastic surface

Biofilms are often utilized by bacteria, often as a means to survive in harsh environments (Yin et al., 2019). To check whether landfill *Brucella* isolates can form biofilms on LLDPE, we performed the CRA assay for biofilm detection (Freeman et al., 1989). Interestingly, the two assay conditions (standard vs modified) produced markedly different outcomes in biofilm assessment (*SI Figure 3*). Under standard CRA conditions (No nutrient source like BHI), neither isolate demonstrated any black pigmentation or precipitation, indicating the absence of biofilm formation in the presence of conventional nutrients. However, a significant shift in biofilm phenotype was observed when the isolates were cultured on the modified CRA with hexadecane. Both isolates showed evidence of

biofilm formation, as confirmed by the appearance of black pigmentation and precipitates in both agar and broth systems. In this study, hexadecane served as a model compound to mimic LLDPE. As it has a hydrocarbon backbone structure, it closely resembles the alkane-derived monomers found in plastic polymers.

For isolate X, robust growth and extensive black precipitation were visible on both solid and liquid modified media, indicating strong biofilm-producing capacity in the presence of hexadecane (*SI Figure 3A and 3B*). In contrast, isolate Y displayed heterogeneous black precipitation on the agar plate, with growth restricted to regions where hexadecane droplets were visibly accumulated (*SI Figure 3C and 3D*). Despite this patchy distribution in the solid medium, the broth culture of isolate Y showed uniform black coloration, suggesting effective biofilm formation when hexadecane was more bioavailable.

These observations underscore a key adaptive behavior: both isolates appear to form biofilms preferentially under hydrocarbon-substituted, nutrient-limited conditions, simulating an environment where plastics like LLDPE are the dominant carbon source. The differing patterns of biofilm formation, particularly the scattered black precipitates produced by isolate Y on the solid medium, can be attributed to the low solubility and uneven distribution of hexadecane in agar, which creates localized microenvironments of carbon availability. Isolate Y likely exhibits a dependence on direct hydrocarbon contact for initiating adhesion and biofilm development, resulting in colony formation only in areas where hexadecane droplets accumulated. In contrast, isolate X may possess enhanced hydrophobic surface properties, emulsifying capabilities, or more efficient hydrocarbon uptake systems, allowing it to colonize more uniformly across the medium. These phenotypic differences reflect varying degrees of metabolic or surface-associated adaptations for hydrocarbon utilization and biofilm formation. Moreover, it also suggests different survival strategies: isolate X may rely on stronger emulsification or surface hydrophobic proteins to disperse across the medium, while isolate Y depends more on localized substrate deposits. Similar hydrocarbon-induced biofilm behaviors have been reported in other plastic and alkane-degrading bacteria, such as *Pseudomonas aeruginosa*, *Rhodococcus ruber*, and *Bacillus subtilis*, where contact with hydrophobic substrates triggered enhanced EPS production and adhesion (Das and Chandran, 2011; Skariyachan et al., 2016; Urbanek et al., 2018). Such adaptations are considered advantageous in landfill environments because biofilms not only promote persistence under nutrient limitation but also facilitate close cell–substrate contact, which is critical for enzymatic depolymerization (McFall et al., 2024). This indicates possible genetic or metabolic differences that are further investigated through genomic analysis.

To check the genetic basis of biofilm formation, we checked the genomes of the two isolates against a manually curated set of 63 biofilm-forming genes (*SI Table 3*). Our analysis identified 13 and 12 significant homologs in the *B. intermedia* X and Y landfill isolates, respectively, corresponding to nine unique reference biofilm genes from our curated biofilm dataset. Both genomes displayed a nearly identical homolog profile. The identified homologs were predominantly associated with matrix polysaccharide synthesis and surface adhesion (e.g., *bap*, *pslA*, *algD*) and two-component regulatory systems (*gacA/gacS*-like). However, canonical quorum-sensing regulators such as *lasI/R*, *rhlI/R*, and *agrA/C* were not detected, consistent with

an altered regulatory landscape relative to classical model species. This pattern indicates that the biofilm-forming potential of the environmental isolates may depend more on structural and stress-responsive elements than on quorum-sensing–driven regulation. Overall, the close correspondence between the landfill isolates X and Y suggests a conserved repertoire of biofilm-associated genes within the isolated environmental lineages of *Brucella*. Such conservation likely supports surface persistence and environmental survival, even in the absence of canonical quorum-sensing systems. Sequence-level conservation combined with selective retention of adhesion and exopolysaccharide synthesis genes points to an ecologically adapted biofilm phenotype that may facilitate environmental endurance rather than host-associated colonization.

4. Conclusion

This study provides the first functional and genomic evidence that *Brucella intermedia* can degrade linear low-density polyethylene (LLDPE). Two environmental isolates, X and Y, recovered from a landfill site, exhibited clear signs of LLDPE biodegradation, confirmed by FTIR and SEM analyses. Moreover, genomic profiling revealed an enrichment of enzymes associated with the three key stages of plastic degradation: oxidative activation, depolymerization, and assimilation-mineralization. The dominance of copper oxidase and depolymerase enzymes suggests a coordinated pathway that initiates oxidation of the LLDPE backbone, followed by hydrolytic cleavage and metabolic assimilation of intermediates. Both isolates possessed efflux-based intrinsic resistance and lacked major virulence determinants, indicating that they are environmentally adapted and non-pathogenic. Their ability to form biofilms under hydrocarbon-substituted conditions further supports their ecological competence in polymer-rich habitats. Overall, these findings expand the known taxonomic range of plastic-degrading bacteria and demonstrate that *B. intermedia*, traditionally recognized for their pathogenic potentials, also possesses environmentally relevant degradative functions. Collectively, the data argue for systematic microbiological exploration of plastic-rich niches, with the potential to uncover previously undescribed plastic-degrading species.

Funding

The authors declare that this research did not receive any specific grant from funding agencies in the public, commercial, or not-for-profit sectors. Costs for some of the experiments were provided by the departmental fund of the Department of Mathematics & Natural Sciences, Brac University.

CRediT authorship contribution statement

Ifthikhar Zaman: Writing – original draft, Writing – review & editing, Validation, Methodology, Investigation, Formal analysis, Data curation, Conceptualization, Visualization. Mahdi Muhammad Moosa: Writing – original draft, Writing – review & editing, Validation, Methodology, Investigation, Conceptualization, Visualization, Formal analysis, Data curation. M. Mahboob Hossain: Writing – review & editing, Validation, Supervision.

Declaration of competing interest

The authors declare that they have no known competing financial interests or personal relationships that could have appeared to influence the work reported in this paper.

Declaration of generative AI use

The author(s) used Grammarly and ChatGPT for language editing and ChatGPT, Gemini, and Grok for technical assistance in software setup and data analysis scripting. All content was subsequently reviewed and approved by the author(s), who assume full responsibility for the final manuscript.

Data Availability

All sequencing data generated in this study are available in the ENA Project study accession PRJEB101032.

Acknowledgments

We acknowledge Zwad Al Saiyan for assistance with figure preparation and Sadrina Afrin Mowna for proofreading the manuscript.

References:

Afgan, E., Baker, D., Batut, B., van den Beek, M., Bouvier, D., Čech, M., Chilton, J., Clements, D., Coraor, N., Grüning, B.A., Guerler, A., Hillman-Jackson, J., Hiltemann, S., Jalili, V., Rasche, H., Soranzo, N., Goecks, J., Taylor, J., Nekrutenko, A., Blankenberg, D., 2018. The Galaxy platform for accessible, reproducible and collaborative biomedical analyses: 2018 update. Nucleic Acids Res. 46, W537–W544. https://doi.org/10.1093/nar/gky379

Alamer, N.J., Aldayel, M.F., Khalifa, A., 2023. Isolation and Characterization of Brucella spp., Low-Density Polyethylene (LDPE) Plastic Degrading Bacteria in Al-Ahsa Region, Saudi Arabia. Appl. Sci. 13, 4629. https://doi.org/10.3390/app13074629

Alcock, B.P., Huynh, W., Chalil, R., Smith, K.W., Raphenya, A.R., Wlodarski, M.A., Edalatmand, A., Petkau, A., Syed, S.A., Tsang, K.K., Baker, S.J.C., Dave, M., McCarthy, M.C., Mukiri, K.M., Nasir, J.A., Golbon, B., Imtiaz, H., Jiang, X., Kaur, K., Kwong, M., Liang, Z.C., Niu, K.C., Shan, P., Yang, J.Y.J., Gray, K.L., Hoad, G.R., Jia, B., Bhando, T., Carfrae, L.A., Farha, M.A., French, S., Gordzevich, R., Rachwalski, K., Tu, M.M., Bordeleau, E., Dooley, D., Griffiths, E., Zubyk, H.L., Brown, E.D., Maguire, F., Beiko, R.G., Hsiao, W.W.L., Brinkman, F.S.L., Van Domselaar, G., McArthur, A.G., 2023. CARD 2023: expanded curation, support for machine learning, and resistome prediction at the Comprehensive Antibiotic Resistance Database. Nucleic Acids Res. 51, D690–D699. https://doi.org/10.1093/nar/gkac920

Alvarez-Ortega, C., Olivares, J., Martínez, J.L., 2013. RND multidrug efflux pumps: what are they good for? Front. Microbiol. 4, 7. https://doi.org/10.3389/fmicb.2013.00007

Atanasova, N., Stoitsova, S., Paunova-Krasteva, T., Kambourova, M., 2021. Plastic Degradation by Extremophilic Bacteria. Int. J. Mol. Sci. 22, 5610. https://doi.org/10.3390/ijms22115610

Bahl, S., Dolma, J., Jyot Singh, J., Sehgal, S., 2021. Biodegradation of plastics: A state of the art review. Mater. Today Proc., International Conference on Advanced Materials and Modern Manufacturing 39, 31–34. https://doi.org/10.1016/j.matpr.2020.06.096

Byndloss, M.X., Tsolis, R.M., 2016. Brucella spp. Virulence Factors and Immunity. Annu. Rev. Anim. Biosci. 4, 111–127. https://doi.org/10.1146/annurev-animal-021815-111326

Cai, Z., Li, M., Zhu, Z., Wang, X., Huang, Y., Li, T., Gong, H., Yan, M., 2023. Biological Degradation of Plastics and Microplastics: A Recent Perspective on Associated Mechanisms and Influencing Factors. Microorganisms 11, 1661. https://doi.org/10.3390/microorganisms11071661

Chamas, A., Moon, H., Zheng, J., Qiu, Y., Tabassum, T., Jang, J.H., Abu-Omar, M., Scott, S.L., Suh, S., 2020. Degradation Rates of Plastics in the Environment. ACS Sustain. Chem. Eng. 8, 3494–3511. https://doi.org/10.1021/acssuschemeng.9b06635

Chen, L., Zheng, D., Liu, B., Yang, J., Jin, Q., 2016. VFDB 2016: hierarchical and refined dataset for big data analysis--10 years on. Nucleic Acids Res. 44, D694-697. https://doi.org/10.1093/nar/gkv1239

Das, N., Chandran, P., 2011. Microbial Degradation of Petroleum Hydrocarbon Contaminants: An Overview. Biotechnol. Res. Int. 2011, 941810. https://doi.org/10.4061/2011/941810

De Coster, W., D'Hert, S., Schultz, D.T., Cruts, M., Van Broeckhoven, C., 2018. NanoPack: visualizing and processing long-read sequencing data. Bioinformatics 34, 2666–2669. https://doi.org/10.1093/bioinformatics/bty149

Freeman, D.J., Falkiner, F.R., Keane, C.T., 1989. New method for detecting slime production by coagulase negative staphylococci. J. Clin. Pathol. 42, 872–874. https://doi.org/10.1136/jcp.42.8.872

Galgali, P., Varma, A.J., Puntambekar, U.S., Gokhale, D.V., 2002. Towards biodegradable polyolefins: strategy of anchoring minute quantities of monosaccharides and disaccharides onto functionalized polystyrene, and their effect on facilitating polymer biodegradation. Chem. Commun. 2884–2885. https://doi.org/10.1039/B209254A

Gambarini, V., Pantos, O., Kingsbury, J.M., Weaver, L., Handley, K.M., Lear, G., 2022. PlasticDB: a database of microorganisms and proteins linked to plastic biodegradation. Database 2022, baac008. https://doi.org/10.1093/database/baac008

Gautam, R., Bassi, A.S., Yanful, E.K., 2007. A review of biodegradation of synthetic plastic and foams. Appl. Biochem. Biotechnol. 141, 85–108. https://doi.org/10.1007/s12010-007-9212-6

Ghatge, S., Yang, Y., Ahn, J.-H., Hur, H.-G., 2020. Biodegradation of polyethylene: a brief review. Appl. Biol. Chem. 63, 27. https://doi.org/10.1186/s13765-020-00511-3

Gorish, B.M.T., Abdelmula, W.I.Y., Sethupathy, S., Dar, M.A., Shahnawaz, Mohd., Zhu, D., 2024. Microbial degradation of polyethylene polymer: current paradigms, challenges, and future innovations. World J. Microbiol. Biotechnol. 40, 399. https://doi.org/10.1007/s11274-024-04211-8

Gupta, K.K., Devi, D., 2020. Characteristics investigation on biofilm formation and biodegradation activities of Pseudomonas aeruginosa strain ISJ14 colonizing low density polyethylene (LDPE) surface. Heliyon 6, e04398. https://doi.org/10.1016/j.heliyon.2020.e04398

Huerta-Cepas, J., Serra, F., Bork, P., 2016. ETE 3: Reconstruction, Analysis, and Visualization of Phylogenomic Data. Mol. Biol. Evol. 33, 1635–1638. https://doi.org/10.1093/molbev/msw046

Jain, C., Rodriguez-R, L.M., Phillippy, A.M., Konstantinidis, K.T., Aluru, S., 2018. High throughput ANI analysis of 90K prokaryotic genomes reveals clear species boundaries. Nat. Commun. 9, 5114. https://doi.org/10.1038/s41467-018-07641-9

Katz, L.S., Griswold, T., Morrison, S.S., Caravas, J.A., Zhang, S., Bakker, H.C. den, Deng, X., Carleton, H.A., 2019. Mashtree: a rapid comparison of whole genome sequence files. J. Open Source Softw. 4, 1762. https://doi.org/10.21105/joss.01762

Khumthong, I., Siripornadulsil, W., Siripornadulsil, S., 2025. Bacteria isolated from soil degrade low-density polyethylene for growth and polyhydroxyalkanoate synthesis. J. Environ. Manage. 380, 125072. https://doi.org/10.1016/j.jenvman.2025.125072

Kolmogorov, M., Yuan, J., Lin, Y., Pevzner, P.A., 2019. Assembly of long, error-prone reads using repeat graphs. Nat. Biotechnol. 37, 540–546. https://doi.org/10.1038/s41587-019-0072-8

Kyaw, B.M., Champakalakshmi, R., Sakharkar, M.K., Lim, C.S., Sakharkar, K.R., 2012. Biodegradation of Low Density Polythene (LDPE) by Pseudomonas Species. Indian J. Microbiol. 52, 411–419. https://doi.org/10.1007/s12088-012-0250-6

Leslie, H.A., van Velzen, M.J.M., Brandsma, S.H., Vethaak, A.D., Garcia-Vallejo, J.J., Lamoree, M.H., 2022. Discovery and quantification of plastic particle pollution in human blood. Environ. Int. 163, 107199. https://doi.org/10.1016/j.envint.2022.107199

Li, S.-Y., Huang, Y.-E., Chen, J.-Y., Lai, C.-H., Mao, Y.-C., Huang, Y.-T., Liu, P.-Y., 2021. Genomics of Ochrobactrum pseudogrignonense (newly named Brucella pseudogrignonensis) reveals a new blaOXA subgroup. Microb. Genomics 7, 000626. https://doi.org/10.1099/mgen.0.000626

Manni, M., Berkeley, M.R., Seppey, M., Simão, F.A., Zdobnov, E.M., 2021. BUSCO Update: Novel and Streamlined Workflows along with Broader and Deeper Phylogenetic Coverage for Scoring of Eukaryotic, Prokaryotic, and Viral Genomes. Mol. Biol. Evol. 38, 4647–4654. https://doi.org/10.1093/molbev/msab199

McFall, A., Coughlin, S.A., Hardiman, G., Megaw, J., 2024. Strategies for biofilm optimization of plastic-degrading microorganisms and isolating biofilm formers from plastic-contaminated environments. Sustain. Microbiol. 1, qvae012. https://doi.org/10.1093/sumbio/qvae012

Nadjar, D., Labia, R., Cerceau, C., Bizet, C., Philippon, A., Arlet, G., 2001. Molecular Characterization of Chromosomal Class C β-Lactamase and Its Regulatory Gene in Ochrobactrum anthropi. Antimicrob. Agents Chemother. 45, 2324–2330. https://doi.org/10.1128/AAC.45.8.2324-2330.2001

Nowak, B., Pająk, J., Drozd-Bratkowicz, M., Rymarz, G., 2011. Microorganisms participating in the biodegradation of modified polyethylene films in different soils under laboratory conditions. Int. Biodeterior. Biodegrad. 65, 757–767. https://doi.org/10.1016/j.ibiod.2011.04.007

Omokhagbor Adams, G., Tawari Fufeyin, P., Eruke Okoro, S., Ehinomen, I., 2020. Bioremediation, Biostimulation and Bioaugmention: A Review. Int. J. Environ. Bioremediation Biodegrad. 3, 28–39. https://doi.org/10.12691/ijebb-3-1-5

Peacock, A., 2000. Handbook of Polyethylene: Structures: Properties, and Applications. CRC Press, Boca Raton. https://doi.org/10.1201/9781482295467

Qureshi, K.A., Parvez, A., Fahmy, N.A., Abdel Hady, B.H., Kumar, S., Ganguly, A., Atiya, A., Elhassan, G.O., Alfadly, S.O., Parkkila, S., Aspatwar, A., 2023. Brucellosis: epidemiology, pathogenesis, diagnosis and treatment–a comprehensive review. Ann. Med. 55, 2295398. https://doi.org/10.1080/07853890.2023.2295398

Ragusa, A., Svelato, A., Santacroce, C., Catalano, P., Notarstefano, V., Carnevali, O., Papa, F., Rongioletti, M.C.A., Baiocco, F., Draghi, S., D'Amore, E., Rinaldo, D., Matta, M., Giorgini, E., 2021. Plasticenta: First evidence of microplastics in human placenta. Environ. Int. 146, 106274. https://doi.org/10.1016/j.envint.2020.106274

Rahimi, A., García, J.M., 2017. Chemical recycling of waste plastics for new materials production. Nat. Rev. Chem. 1, 0046. https://doi.org/10.1038/s41570-017-0046

Rajandas, H., Parimannan, S., Sathasivam, K., Ravichandran, M., Su Yin, L., 2012. A novel FTIR-ATR spectroscopy based technique for the estimation of low-density polyethylene biodegradation. Polym. Test. 31, 1094–1099. https://doi.org/10.1016/j.polymertesting.2012.07.015

Santo, M., Weitsman, R., Sivan, A., 2013. The role of the copper-binding enzyme – laccase – in the biodegradation of polyethylene by the actinomycete *Rhodococcus ruber*. Int. Biodeterior. Biodegrad. 84, 204–210. https://doi.org/10.1016/j.ibiod.2012.03.001

Seemann, T., 2025a. tseemann/snippy.

Seemann, T., 2025b. tseemann/abricate.

Shah, A.A., Hasan, F., Hameed, A., Ahmed, S., 2008. Biological degradation of plastics: A comprehensive review. Biotechnol. Adv. 26, 246–265. https://doi.org/10.1016/j.biotechadv.2007.12.005

Shalem, A., Yehezkeli, O., Fishman, A., 2024. Enzymatic degradation of polylactic acid (PLA). Appl. Microbiol. Biotechnol. 108, 413. https://doi.org/10.1007/s00253-024-13212-4

Shen, W., Sipos, B., Zhao, L., 2024. SeqKit2: A Swiss army knife for sequence and alignment processing. iMeta 3, e191. https://doi.org/10.1002/imt2.191

Singh, G., Kaur, N., Bhunia, H., Bajpai, P.K., Mandal, U.K., 2012. Degradation behaviors of linear low-density polyethylene and poly(L-lactic acid) blends. J. Appl. Polym. Sci. 124, 1993–1998. https://doi.org/10.1002/app.35216

Skariyachan, S., Manjunatha, V., Sultana, S., Jois, C., Bai, V., Vasist, K.S., 2016. Novel bacterial consortia isolated from plastic garbage processing areas demonstrated enhanced degradation for low density polyethylene. Environ. Sci. Pollut. Res. 23, 18307–18319. https://doi.org/10.1007/s11356-016-7000-y

Socrates, G., 2004. Infrared and Raman Characteristic Group Frequencies: Tables and Charts. John Wiley & Sons.

Srivastava, P., Singh, S., Soni, M., Pratap, J.V., Subramanian, S., Manickam, N., 2025. Enzymatic degradation of PET by hydrolase from Brucella intermedia IITR130 and its genomic insights. Biodegradation 36, 45. https://doi.org/10.1007/s10532-025-10141-5

Taghavi, N., Singhal, N., Zhuang, W.-Q., Baroutian, S., 2021. Degradation of plastic waste using stimulated and naturally occurring microbial strains. Chemosphere 263, 127975. https://doi.org/10.1016/j.chemosphere.2020.127975

Thirumalaivasan, N., Gnanasekaran, L., Kumar, S., Durvasulu, R., Sundaram, T., Rajendran, S., Nangan, S., Kanagaraj, K., 2024. Utilization of fungal and bacterial bioremediation techniques for the treatment of toxic waste and biowaste. Front. Mater. 11. https://doi.org/10.3389/fmats.2024.1416445

Urbanek, A.K., Rymowicz, W., Mirończuk, A.M., 2018. Degradation of plastics and plastic-degrading bacteria in cold marine habitats. Appl. Microbiol. Biotechnol. 102, 7669–7678. https://doi.org/10.1007/s00253-018-9195-y

Wood, D.E., Lu, J., Langmead, B., 2019. Improved metagenomic analysis with Kraken 2. Genome Biol. 20, 257. https://doi.org/10.1186/s13059-019-1891-0

Yin, W., Wang, Y., Liu, L., He, J., 2019. Biofilms: The Microbial "Protective Clothing" in Extreme Environments. Int. J. Mol. Sci. 20, 3423. https://doi.org/10.3390/ijms20143423

Yoshida, S., Hiraga, K., Takehana, T., Taniguchi, I., Yamaji, H., Maeda, Y., Toyohara, K., Miyamoto, K., Kimura, Y., Oda, K., 2016a. A bacterium that degrades and assimilates poly(ethylene terephthalate). Science 351, 1196–1199. https://doi.org/10.1126/science.aad6359

Yoshida, S., Hiraga, K., Takehana, T., Taniguchi, I., Yamaji, H., Maeda, Y., Toyohara, K., Miyamoto, K., Kimura, Y., Oda, K., 2016b. A bacterium that degrades and assimilates poly(ethylene terephthalate). Science 351, 1196–1199. https://doi.org/10.1126/science.aad6359

Zaman, I., Turjya, R.R., Shakil, M.S., Al Shahariar, M., Md. Rezanur Rahman, H.E., Ahmed, A., Hossain, M.M., 2024. Biodegradation of polyethylene and polystyrene by Zophobas atratus larvae from Bangladeshi source and isolation of two plastic-degrading gut bacteria. Environ. Pollut. 123446. https://doi.org/10.1016/j.envpol.2024.123446

Zampolli, J., Mangiagalli, M., Vezzini, D., Lasagni, M., Ami, D., Natalello, A., Arrigoni, F., Bertini, L., Lotti, M., Di Gennaro, P., 2023. Oxidative degradation of polyethylene by two novel laccase-like multicopper oxidases from *Rhodococcus opacus* R7. Environ. Technol. Innov. 32, 103273. https://doi.org/10.1016/j.eti.2023.103273

Zankari, E., Hasman, H., Cosentino, S., Vestergaard, M., Rasmussen, S., Lund, O., Aarestrup, F.M., Larsen, M.V., 2012. Identification of acquired antimicrobial resistance genes. J. Antimicrob. Chemother. 67, 2640–2644. https://doi.org/10.1093/jac/dks261

Graphical Abstract

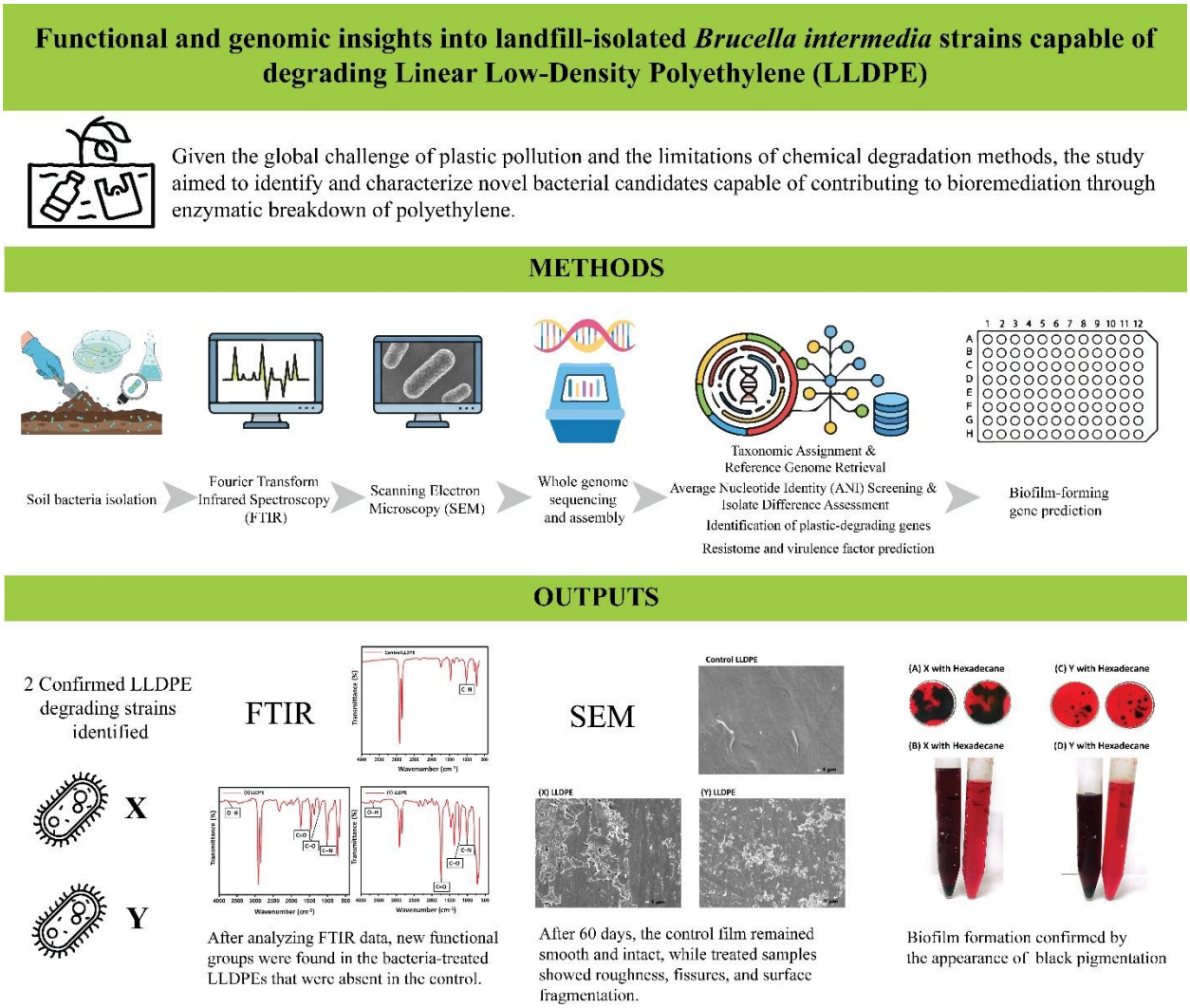

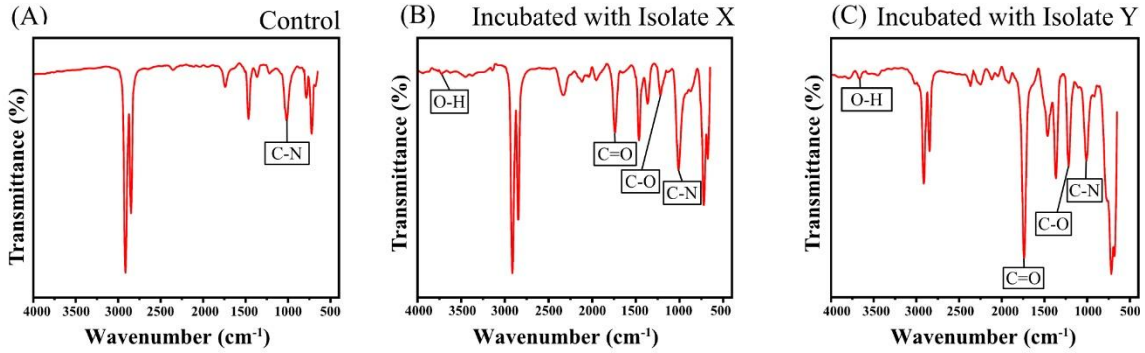

Figure 1: Fourier Transform Infrared (FTIR) Spectra showing formation of distinct functional groups in treated linear low-density polyethylene (LLDPE) strips with landfill isolates X and Y. (**A**) Control LLDPE exhibited only the characteristic C–H stretching and a weak band at ~1020 cm^{-1} (C–N stretch) that is likely a polymer additive or processing residues. (**B**) LLDPE strip treated with isolate X. New functional groups found at 1550-1720 cm^{-1} (C=O stretch), 1250–1300 cm^{-1} (C─O stretch), and 3000-3670 cm^{-1} (O─H stretch), indicating oxidation. (**C**) LLDPE strip treated with isolate Y. Similar new functional groups were found, similar to X.

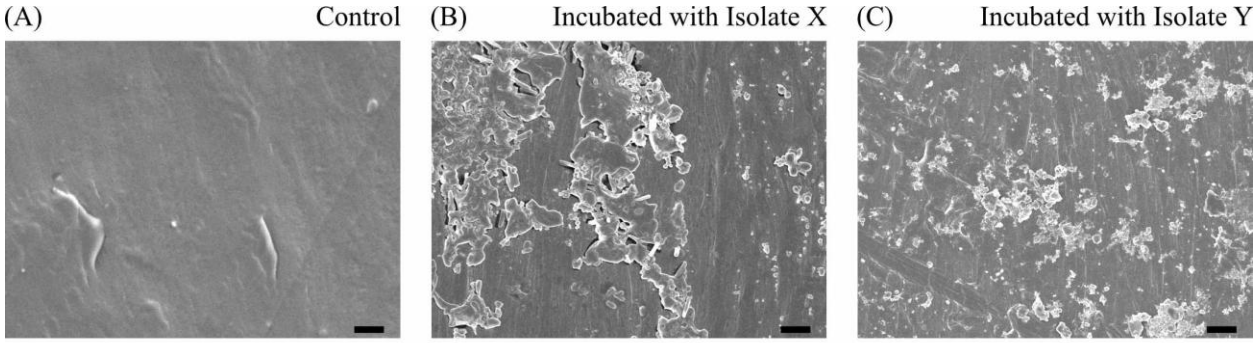

Figure 2: Scanning electron microscopy (SEM) images of treated and untreated LLDPE strips. (**A**) Control untreated LLDPE strip showing smooth intact surface, consistent with the absence of any degradation. LLDPE strips treated with isolate X (**B**) and isolate Y (**C**) showing clear degradation signatures, including roughened textures, fissures, and surface fragmentation. Scale bars represent 3 µm.

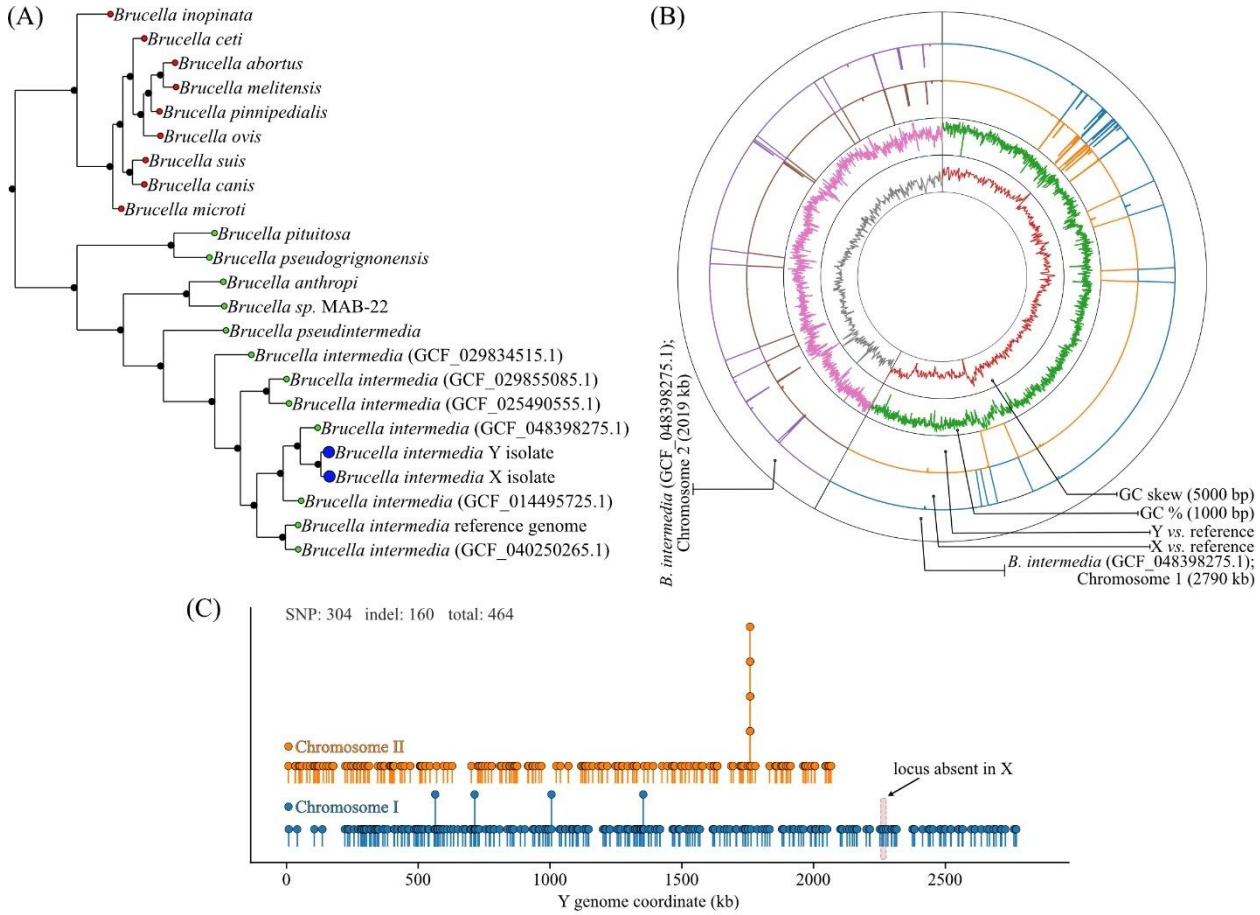

Figure 3: (**A**) *Isolates X and Y cluster with environmental Brucella intermedia clades.* Whole-genome phylogeny of the *Brucella* genus. Environmental species (green-filled circle at the tip) and pathogenic species (red-filled circle at the tip) form distinct clades; isolates X and Y (blue-filled large circle at the tip) cluster with *B. intermedia*. Tree visualized with a custom root for clarity and square-root-scaled branch lengths. (**B**) *Landfill isolates are distinct from their nearest sequenced B. intermedia neighbor.* Circos plot: reference genome (outer ring), read depth from isolates X and Y (middle rings), and GC metrics (inner rings). White gaps in the X/Y rings mark "accessory genomic islands" that are present in the hospital-wastewater reference but missing from one or both landfill isolates. (**C**) *X and Y isolates are genomically distinct.* Genome-wide single nucleotide polymorphisms (SNPs) and small indels between isolates X and Y (visualized using isolate Y genome as the reference). Variants were visualized as stacked lollipop plots across the two chromosomes, where vertical offset markers represent overlapping or closely spaced variants (pile-ups). A ~19.8 kb region, exclusive to isolate Y and absent in isolate X, is delineated by the red-shaded box.

Table 1: Comparative profile of plastic-degrading enzyme categories in reference *Brucella* genomes (n = 231) and the environmental isolates X and Y. Mean and standard deviation values are based on 231 reference genomes. Counts for X and Y indicate the number of detected homologs per genome. Z-scores represent deviations from the reference mean, highlighting enzymes enriched or depleted in the isolates.

		Reference *Brucella* genomes (n=231)		**Count**		**Z-score**	
Enzyme Category	**Enzyme**	**Mean**	**Standard Deviation**	**X**	**Y**	**X**	**Y**
Oxidative activation	Copper oxidase	0.01	0.11	1	1	8.7	8.7
	Laccase	0.03	0.16	0	0	-0.16	-0.16
Depolymerization	PHA depolymerase	0.04	0.19	0	0	-0.2	-0.2
	PLA depolymerase	1	0	1	1		
	PU esterase	0	0.07	0	0	-0.07	-0.07
	Polyamidase	0.1	0.37	1	1	2.46	2.46
	Polyesterase	1	0	1	1	-	-
Assimilation-mineralization	3HV dehydrogenase	13.45	3.77	20	20	1.74	1.74
	Carboxylesterase	0.03	0.16	0	0	-0.16	-0.16
	Hydrolase	0.62	0.49	0	0	-1.28	-1.28
	Lipase	0.21	0.75	0	0	-0.28	-0.28
	Nylon Oligomer Degrading Enzyme	1.25	0.5	1	1	-0.5	-0.5
	Nylon hydrolase	0.03	0.16	0	0	-0.16	-0.16
	PEG aldehyde dehydrogenase	13.01	0.89	13	13	-0.01	-0.01
	PEG dehydrogenase	4.69	0.66	4	4	-1.04	-1.04

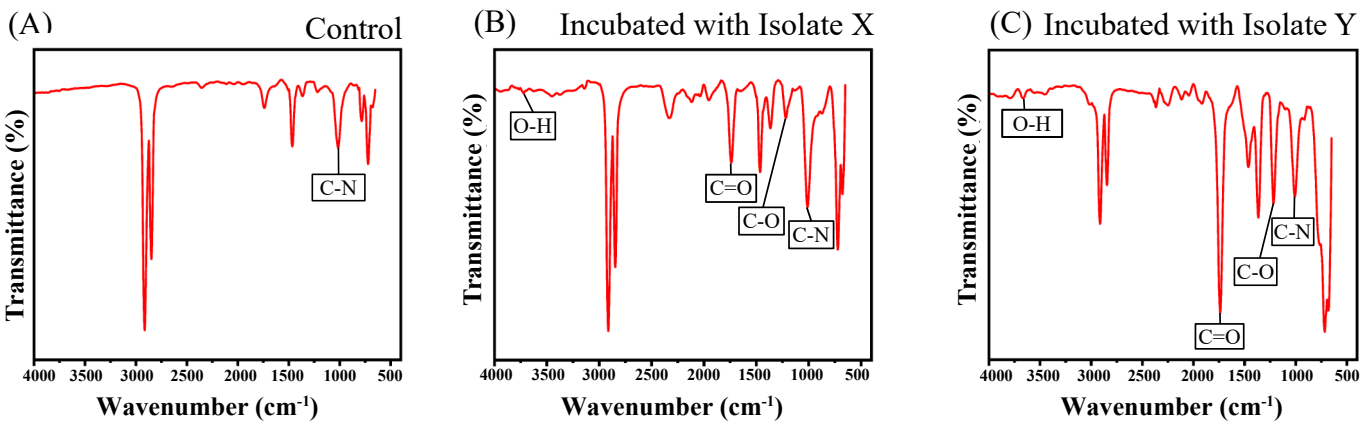
(A)
Control
C-N
Transmittance (%)
4000 3500 3000 2500 2000 1500 1000 500
Wavenumber (cm-1)
(B)
Incubated with Isolate X
O-H
C=O
C-O
C-N
Transmittance (%)
4000 3500 3000 2500 2000 1500 1000 500
Wavenumber (cm-1)
(C)
Incubated with Isolate Y
O-H
C-N
C-O
C=O
Transmittance (%)
4000 3500 3000 2500 2000 1500 1000 500
Wavenumber (cm-1)

(A) Control

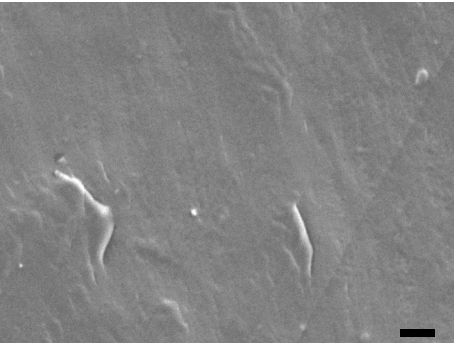

(B) Incubated with Isolate X

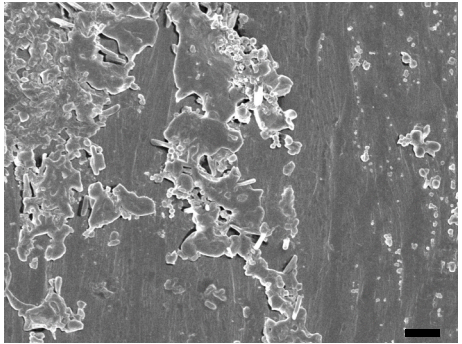

(C) Incubated with Isolate Y

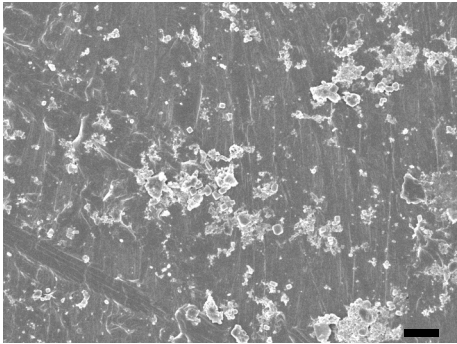

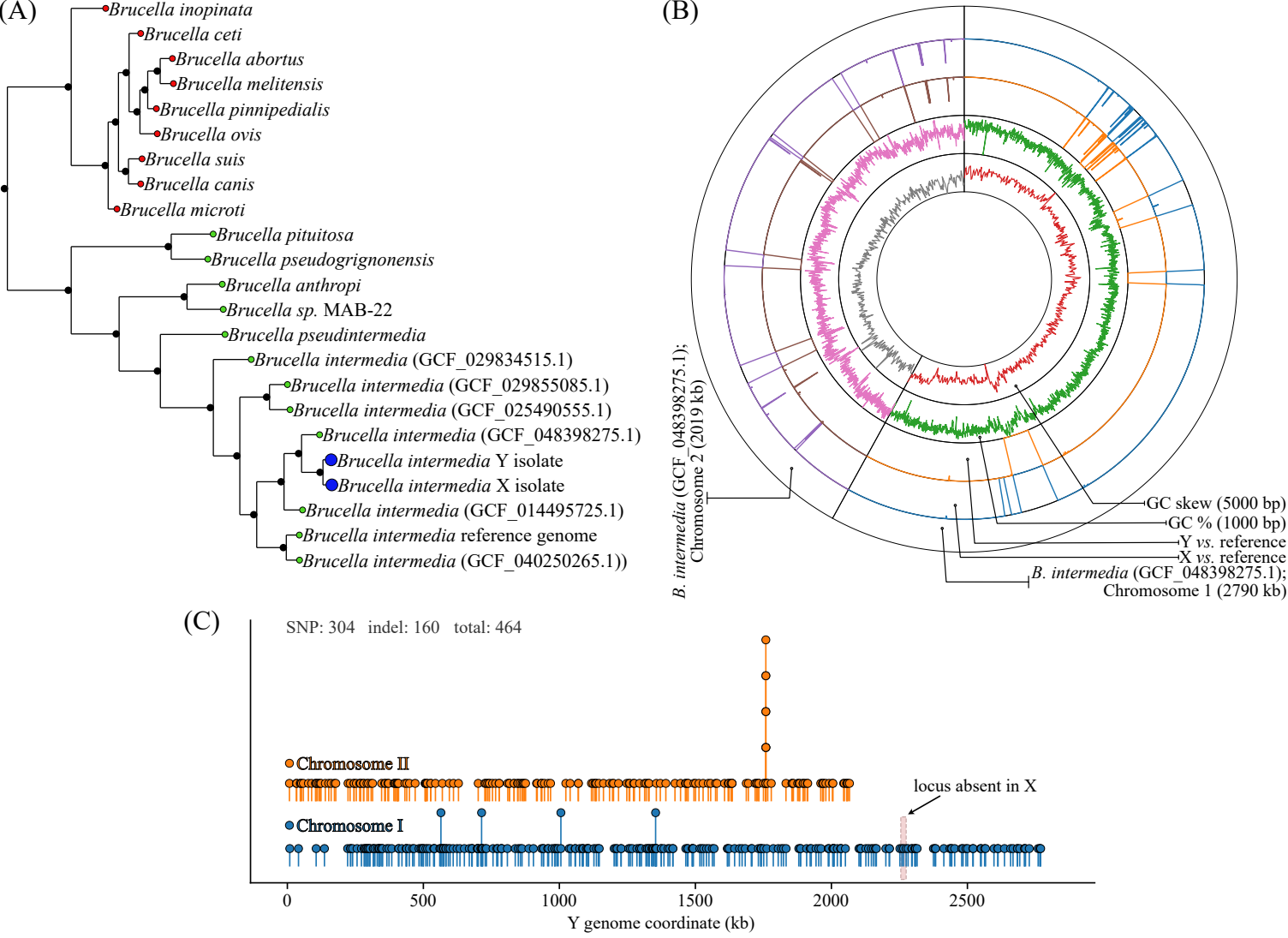
(A)
Brucella inopinata
Brucella ceti
Brucella abortus
Brucella melitensis
Brucella pinnipedialis
Brucella ovis
Brucella suis
Brucella canis
Brucella microti
Brucella pituitosa
Brucella pseudogrignonensis
Brucella anthropi
Brucella sp. MAB-22
Brucella pseudintermedia
Brucella intermedia (GCF_029834515.1)
Brucella intermedia (GCF_029855085.1)
Brucella intermedia (GCF_025490555.1)
Brucella intermedia (GCF_048398275.1)
Brucella intermedia Y isolate
Brucella intermedia X isolate
Brucella intermedia (GCF_014495725.1)
Brucella intermedia reference genome
Brucella intermedia (GCF_040250265.1))
(B)
B. intermedia (GCF_048398275.1); Chromosome 2 (2019 kb)
GC skew (5000 bp)
GC % (1000 bp)
Y vs. reference
X vs. reference
B. intermedia (GCF_048398275.1); Chromosome 1 (2790 kb)
(C)
SNP: 304 indel: 160 total: 464
Chromosome II
Chromosome I
locus absent in X
0
500
1000
1500
2000
2500
Y genome coordinate (kb)